

Density Functional Theory Studies on Chemical Functionalization of Single-Walled Carbon Nanotubes by Bingel Reaction

Tomokazu Umeyama,[1] Hiroyuki Fueno,[1] Eisuke Kawabata,[1] Yoshikazu Kobayashi,[1] Kazuyoshi Tanaka,*[1] Noriyasu Tezuka,[1] Yoshihiro Matano,[1] and Hiroshi Imahori*[1,2,3]

[1]Department of Molecular Engineering, Graduate School of Engineering, Kyoto University, Nishikyo-ku, Kyoto 615-8510

[2]Institute for Integrated Cell-Material Sciences (iCeMS), Kyoto University, Nishikyo-ku, Kyoto 615-8510

[3]Fukui Institute for Fundamental Chemistry, Kyoto University, 34-4 Takano-Nishihiraki-cho, Sakyo-ku, Kyoto 606-8103

Received November 19, 2010; E-mail: imahori@scl.kyoto-u.ac.jp, ktanaka@moleng.kyoto-u.ac.jp

Theoretical investigations on single-walled carbon nanotubes (SWNTs) functionalized by Bingel reaction were conducted using finite-length models based on density functional theory. The electronic structures of the adduct with Type 1 configuration, where the circumferential C–C bonds in sidewall are reacted with a malonate anion, are largely retained after the functionalization owing to the sidewall opening at the C–C bond between the bridgehead carbons. In contrast, Type 2 configurations, where the axial C–C bonds are the reaction sites, cause significant change in the electronic structures. Taking into account the experimental results that the electronic properties of SWNTs are largely maintained, Type 1 configurations are formed selectively. In addition, calculations on energies of transition states, intermediates, and products suggest that Type 1 geometry is thermodynamically favorable but kinetically unfavorable compared to Type 2. This indicates the occurrence of isomerization from Type 2 to Type 1 after the Bingel reaction, attaining both of the preservation of electronic structure and the improvement of solubility with the high concentration of the addend group.

Single-walled carbon nanotubes (SWNTs) are current targets of general interest for their unique optical, electronic, thermal, and mechanical properties, particularly in connection with applications in various molecular devices.[1–3] However, the poor dispersibility of SWNTs due to the bundle formation in organic and aqueous solvents has hindered solution-phase processing. Covalent functionalizations[4–19] and supramolecular modifications[20–22] of SWNTs provide a facile method to access SWNT derivatives with lower tendency to form bundles and better dispersion capabilities in solution as well as additional functionalities. A variety of reactants such as azomethine ylides[6–8] and aryl radicals[9,10] have been utilized previously to effect covalent modifications at the sidewalls of the SWNT. It must be noted, however, that the covalent functionalization of the SWNT sidewall causes an increase in saturation on the nanotube surface, which involves the formation of saturated sp^3 bonds on the nanotube surface. Point changes in the hybridization of sidewall atoms from sp^2 to sp^3 results in significant alternations of the electronic properties of the nanotube, when compared to pristine SWNTs. Therefore, it is a challenge to exploit covalent modification method that allows us to achieve retention of the intrinsic electronic properties as well as sufficient solubility of SWNTs after covalent functionalization.

One of the most successful methods reported for the covalent functionalization of SWNTs is the reaction of a dichlorocarbene with pristine SWNTs to form dichloromethylene addends that bridge two carbon atoms of the nanotube sidewall.[11–13] Theoretical investigations predicted that the dichloromethylene adduct adopts two different configurations along the nanotube sidewall.[14–19] The first type is a closed configuration, where a cyclopropane ring is formed on the nanotube sidewall. The second is an open configuration, in which the dichloromethylene moiety is adsorbed on an open site on the nanotube created by a rupture of the bottom C–C bond in the sidewall. The addition reactions at the circumferential C–C bonds in the sidewall form the open configuration, while axial C–C bonds undergo the cyclopropanation (closed configuration).[14–19] Recent theoretical studies indicated that if sidewall modification at the ratio of one carbene per ca. 100 sidewall carbons, and the modifications occurred via the open configuration, the electronic structure and the electrical conductance of pristine SWNTs are preserved upon sidewall functionalization.[23,24] However, the present synthetic methodology available makes it difficult to achieve the required addend conformation to promote the open configuration.

Another example of methylene additions onto SWNT sidewalls is the nucleophilic cycloaddition of the malonate carbanion, namely the Bingel reaction. This particular reaction was initially applied for the introduction of functionality onto C_{60} fullerenes[25,26] and recently to SWNTs.[27–29] Our recent experimental study on the sidewall functionalization of SWNTs using the Bingel reaction revealed that the degree of the sidewall functionalization (one addend per 75–300 carbon atoms of SWNTs) was controllable by changing the output power of microwave heating in the synthetic procedure.[29] Of greater significance, it was found that the electronic properties

Published on the web June 25, 2011; doi:10.1246/bcsj.20100326

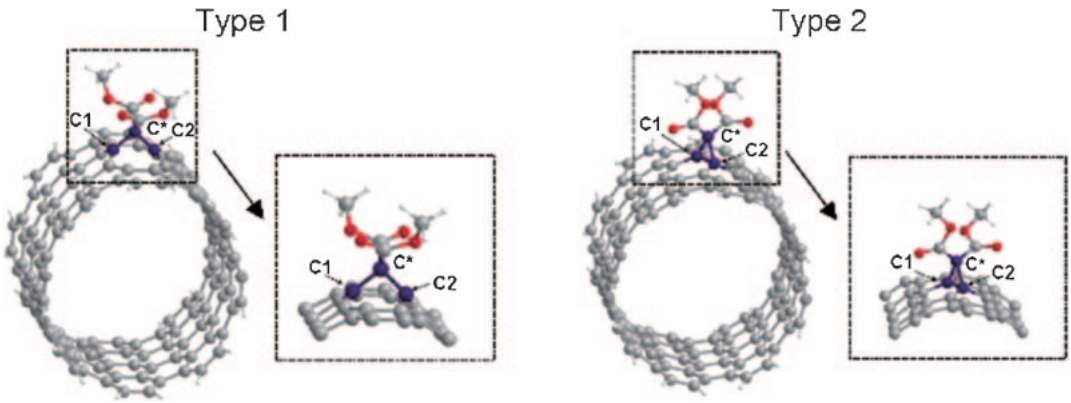

Figure 1. Optimized geometry of the (8,8) nanotube models functionalized by Bingel reaction.

of SWNTs were largely unperturbed after the sidewall modification procedure via the microwave-assisted Bingel reaction.[29] This result is in remarkable contrast with the dichlorocarbene addition reaction (one addend per 100 carbon atoms of SWNTs), which resulted in the loss of the electronic properties of the SWNT.[11] Although the sole theoretical study on site-selectivity of double cyclopropanation reactions was recently reported,[30] systematic theoretical investigations to enable comparisons of the theoretical data with experimental results of Bingel reaction using SWNTs have yet to be conducted.

Herein, we report the first theoretical investigations on the electronic structure of SWNT models functionalized via the Bingel reaction using dimethyl malonate through the use of density functional theory (DFT) calculations. The outcomes of the theoretical studies are compared with previously obtained experimental results for the first time.[29] Likewise the addition reaction of dichlorocarbene,[11–19] it was revealed that the binding configurations of the dimethyl malonate with respect to the tube axis is a critical factor to control in order to preserve the electronic structure of the SWNT. In addition to this, the reaction pathway of the Bingel reaction[31] was studied using theoretical SWNT models with different binding configurations of malonates on the SWNT models. Although the energy profiles for the dichlorocarbene addition was already reported,[16] those for the malonate anion addition to SWNT sidewalls have not been investigated so far.

Computational Details

We chose (8,8) armchair and the (10,5) chiral tubes as representative examples in this study because resonant Raman spectra revealed the involvement in SWNT samples used in previous experimental investigations.[29] The (8,8) and (10,5) SWNTs have similar diameters of ca. 1.1 nm with metallic and semiconducting characters, respectively.[32] Finite-length nanotubes terminated by H atoms were employed as the models for the pristine (8,8) and (10,5) SWNTs ($C_{144}H_{30}$ and $C_{140}H_{32}$, respectively). Dimethyl malonate was used as the addend, in place of benzyl 2-ethylhexyl malonate used in the experimental study,[29] in order to simplify the models. Although iodine reacted with benzyl 2-ethylhexyl malonate in the presence of base to produce the corresponding α-iodomalonate anion in an experimental study,[29] we chose to employ the dimethyl chloromalonate carbanion instead of the iodomalonate carbanion as the substrate of the Bingel reaction for the theoretical investigation on the reaction mechanism, in order to reduce the calculation cost.

In the (8,8) nanotube, there are two types of C–C bonds that can participate in the cyclopropanation reaction, the difference being that they are either perpendicular or slanted to the axis of the nanotube. The (10,5) fragment also provides circumferential and axial C–C bonds as reaction sites. For convenience, we label the SWNTs functionalized at perpendicular and circumferential C–C bonds as Type 1 and SWNTs reacted at the slanted and axial bonds as Type 2. The models of SWNTs functionalized by Bingel reaction in this study possess one malonate group at the center of the fragment sidewall.

The geometry optimizations and electronic structure calculations of the SWNT models were performed using B3LYP functional and 3-21G basis set implemented in Gaussian03 program package.[33] All minima were characterized to have zero imaginary frequency, and all transition states show only one imaginary frequency. Molecular orbitals were visualized by MolStudio R4.0, NEC Corporation, 2004. In contrast to the study on the dichlorocarbene addition,[16] we have taken into account the solvent effect to estimate the energies of the anionic compounds properly by single-point energy calculations with the polarizable continuum model (PCM)[34] with the B3LYP/3-21G method using the optimized geometries obtained at the same level of theory (B3LYP/3-21G). We used chlorobenzene, of which data are implemented in the Gaussian 03 program package, for the solvent effect calculation due to the resemblance of the structure with *o*-dichlorobenzene used as the reaction medium in the experimental study.[29] B3PW91/PCM/3-21G was also employed for the single-point energy calculations.

Results and Discussion

Structures, Formation Energies, and Electronic Properties. The optimized structures of the (8,8) and (10,5) nanotube models functionalized by Bingel reaction with Type 1 and 2 configurations were calculated at the B3LYP/3-21G level and are depicted in Figure 1 and Figure S1 (Supporting Information), respectively. The binding geometries are quite different for the respective binding types as reported for the addition of dichlorocarbene to SWNTs.[14–19] Table 1 lists the computed

Table 1. Characteristic Bond Lengths and Formation Energies of the Nanotube Models Functionalized by Bingel Reaction

SWNT	Type	d_{C1-C2}/Å	d_{C1-C*}/Å	E_f/kcal mol^{-1}
(8,8)	1	2.23	1.53	24.1[a] (29.0)[b]
(8,8)	2	1.57	1.57	15.1[a] (16.4)[b]
(10,5)	1	2.21	1.49	27.4[a] (29.0)[b]
(10,5)	2	1.56	1.54	6.1[a] (13.2)[b]

a) Single point energies were computed in chlorobenzene at the B3LYP/3-21G level of theory. b) Single point energies were computed in chlorobenzene at the B3PW91/3-21G level of theory.

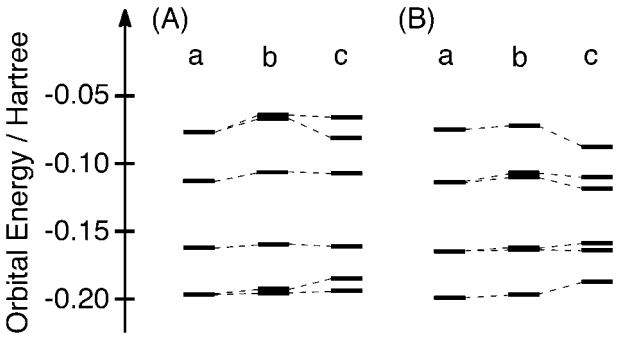

Figure 2. Orbital energy diagrams of (A) (8,8) and (B) (10,5) nanotube models for (a) pristine, (b) Type 1, and (c) Type 2.

characteristic bond lengths between the two carbon atoms to which the addend is attached (d_{C1-C2}) and between the bridged carbon atom and one the addend is attached (d_{C1-C*}), as defined in Figure 1. In both of the (8,8) and (10,5) models, d_{C1-C2} values in Type 2 configuration (1.56–1.57 Å) are rather comparable to the C–C bond length in the pristine (8,8) and (10,5) nanotube models (1.43–1.44 Å). This suggests that Type 2 configurations favor the closed three-membered ring structure. On the other hand, Type 1 configurations result in the d_{C1-C2} separation of ≈2.2 Å, indicating the opened sidewall structure of nanotubes, which is in sharp contrast with selective formation of 6,6-closed adducts in C_{60}.[25,26] This different behavior in Type 1 and Type 2 can be attributed to the large curvature of (8,8) and (10,5) SWNT sidewalls with small diameter (≈1.1 nm). The sidewall opening has significant effects on the electronic structures of the functionalized nanotubes (vide infra).

To assess the adsorption energies of the $C(CO_2Me)_2$ group on the sidewall of SWNTs, we consider the reaction between the pristine nanotube models and dimethyl α-chloromalonate anion, $CCl(CO_2Me)_2^-$. The formation energies (E_f) of SWNT–$C(CO_2Me)_2$ are defined as $E_f = E[\text{SWNT}] + E[CCl(CO_2Me)_2^-] - E[\text{SWNT–C}(CO_2Me)_2] - E[Cl^-]$, where E[SWNT], $E[CCl(CO_2Me)_2^-]$, E[SWNT–$C(CO_2Me)_2$], and $E[Cl^-]$ correspond to the total energies including the solvent effects of the nanotube models, dimethyl chloromalonate anion, the adduct, and chloride ion. Table 1 summarizes the values of E_f calculated at the B3LYP/3-21G level and shows a strong dependence between the formation energy and the binding configuration. Specifically, Type 1 geometries were found to be more thermodynamically favorable than Type 2 in both (8,8) and (10,5) nanotube models, in the same manner for the addition of dichlorocarbene to SWNTs.[14–19] This trend was also corroborated by the E_f values computed using B3PW91 functional instead of B3LYP for the single-point energy calculations (Table 1).

Figure 2 displays the orbital energy diagrams of the nanotube models functionalized by Bingel reaction as well as the pristine nanotubes. In both (8,8) and (10,5) nanotube models, the addition of dimethyl malonate with Type 2 configuration makes a significant change in the orbital energies, as well as orbital splitting, whereas Type 1 binding causes little effect on the orbital energies of the pristine nanotubes. Furthermore, the plots for HOMO, HOMO−1 (the lower-lying orbital below HOMO), and HOMO−2 (the lower-lying orbital below HOMO−1) of the functionalized (8,8) nanotube with Type 1 configuration reveal the orbital lobes spread symmetrically throughout the tube, as in the case of the pristine tube (Figure 3). In contrast, the lobes in Type 2 geometry are less symmetrically distributed (Figure 3) than those in Type 1. The difference in the orbital contour distribution appears to be dependent on the adduct configurations and is consistent with the orbital energy diagrams (Figure 2). Thus, we can safely conclude that SWNTs functionalized by Bingel reaction with Type 1 configuration largely preserve the electronic structures of the pristine nanotubes.[14–19,23] This preservation in Type 1 configuration may stem from the recovery of the sp^2 hybridization on the nanotube sidewall by the bond cleavage between the bottom carbons. More importantly, the malonate group should be added selectively with thermodynamically favorable Type 1 configurations, considering the experimental results that the electronic properties of the corresponding functionalized SWNTs are largely preserved after Bingel reaction.[29]

Energy Profiles for the Addition of $CCl(CO_2Me)_2^-$ to the Nanotube Models. As proposed for the mechanism of the Bingel reaction using fullerenes,[25,26] the reaction mechanism using SWNTs can be considered as follows. First, $CX(CO_2R)_2^-$ (X = halogen) reacts with the electron-deficient π-electron system of SWNTs in a nucleophilic addition manner to yield an intermediate $[\text{SWNT}]^-$–$CX(CO_2R)_2$. Then, the generated carbanion at the sidewall causes intramolecular substitution of the halogen to form a cyclopropane ring structure. In the case of Type 1 configuration, the C–C bond between the bottom carbons at sidewall is cleaved simultaneously. There are various plausible pathways for the selective formation of thermodynamically favorable Type 1 configuration (i.e., the exclusive formation of Type 1 geometry by the Bingel reaction, the occurrence of the rearrangement from Type 2 to Type 1 after the nonselective formation of both configurations, etc.). Note that the addition of diazo compounds to C_{60} yielded kinetically favorable methanofullerenes with [6,5]-open geometry, and the subsequent heating caused the thermal rearrangement to afford the thermodynamically more stable [6,6]-closed isomers.[35,36] To shed light on the reaction process of Bingel reaction using SWNTs, studies on reaction transition states and intermediates are required. Therefore, the energy profiles for the addition of $CCl(CO_2Me)_2^-$ to the (8,8) and (10,5) nanotube models are investigated here.

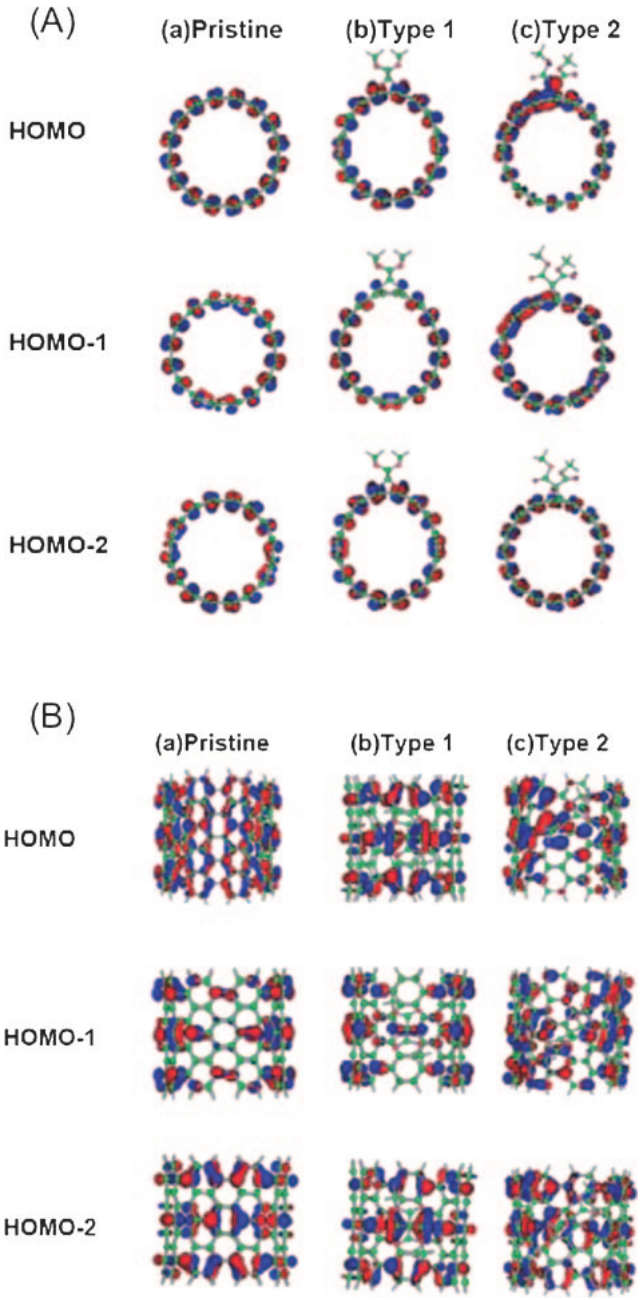

Figure 3. Molecular orbitals corresponding to HOMO, HOMO−1, and HOMO−2 of the (8,8) nanotube model for (a) pristine, (b) Type 1, and (c) Type 2. (A) Side view and (B) top view from the reaction sites.

Figures 4 and 5 exhibit the schematic energy profile and the structures of transition states and intermediates, respectively, for the addition of the geometrically optimized $CCl(CO_2Me)_2^-$ to the C–C bond of the (8,8) nanotube. The calculations were conducted at the B3LYP/3-21G and B3LYP/PCM/3-21G levels for geometry optimizations and single-point energies. The first transition state (TS1) is encountered on approach of $CCl(CO_2Me)_2^-$ to the C–C bond of the (8,8) nanotube. The energy of TS1 is higher by ca. 6 kcal mol^{-1} with respect to the separated reactants. The next stationary point along the reaction path is the intermediate IM, which is characterized by the short

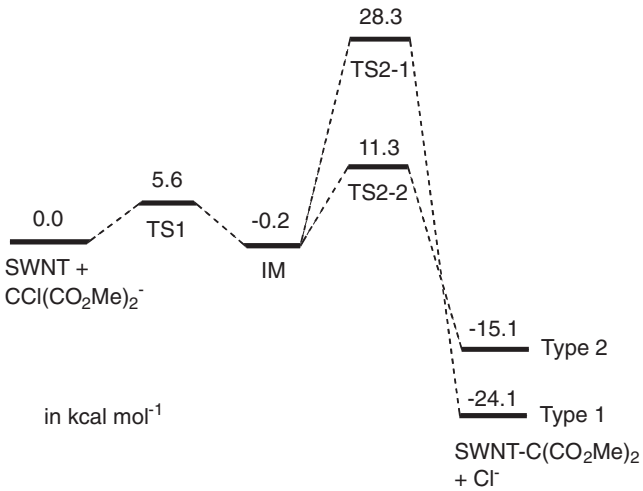

Figure 4. Schematic energy profile (kcal mol^{-1}) for the addition of $CCl(CO_2Me)_2^-$ to the C–C bond of the (8,8) nanotube with Type 1 and Type 2 configurations. Geometry optimizations were performed in the gas phase at the B3LYP/3-21G level of theory; single point energies were computed in chlorobenzene at the B3LYP/PCM/3-21G level.

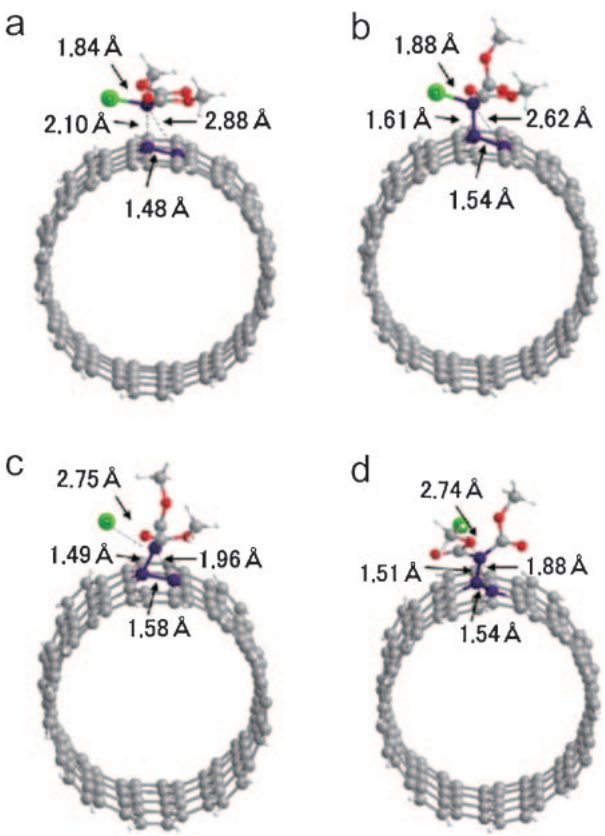

Figure 5. Structures of transition states and intermediates for the addition of $CCl(CO_2Me)_2^-$ to the C–C bond of the (8,8) nanotube. (a) TS1, (b) IM, (c) TS2-1, and (d) TS2-2.

C1–C* bond of 1.61 Å, suggesting the bond formation. The energy of IM is comparable to the separated reactants. Finally, there are additional transition states TS2-1 and TS2-2 toward

the product with Type 1 and Type 2 configurations, respectively, where the ring-closure reactions and the leaving chloride anion occur. The bond length between bottom carbons (d_{C1-C2}) in TS2-1 (1.58 Å) is still comparable to those in IM and TS2-2 (1.54 Å). It is noteworthy that the barrier height from IM to TS2-1 (28.5 kcal mol^{-1}) is much higher than that from IM to TS2-2 (11.5 kcal mol^{-1}), suggesting the kinetically unfavorable formation of the Type 1 configuration. Similarly, the higher activation energy from the intermediate to the second transition state toward Type 1 configuration is predicted for the reaction between $CCl(CO_2Me)_2^-$ and the (10,5) nanotube model (Figure S2 and Figure S3, Supporting Information). Furthermore, the higher activation energy toward Type 1 was also supported by the energy profiles computed using B3PW91 functional instead of B3LYP for single-point energy calculations (Figure S4, Supporting Information).

These theoretical investigations provide valuable insight into the previous experimental results of Bingel reaction using SWNTs.[29] In the experiments, we used partially soluble SWNTs (a-SWNT), which were prepared by acid treatment and the subsequent formation of amide linkages between alkylamine and carboxy group at the tips and defect sites. Bingel reaction using a-SWNT at room temperature for 24 h yielded modified SWNTs with the functionalization ratio of one malonate unit per 270 carbon atoms of SWNT sidewall. The low addend density at the sidewall may rationalize the small change in the electronic structure after the reaction. On the other hand, microwave heating of the reaction mixture shortened the reaction time to less than 30 min and improved functionalization ratio up to one malonate unit per 75 carbon atoms of SWNTs.[29] Although the mechanism of SWNT–microwave interactions remains incompletely understood, it is known that SWNTs absorb microwaves strongly, producing intense local heating.[37] Therefore, SWNTs may possess sufficiently large energy to surmount the energy barriers for the second transition state under the microwave heating conditions. This promoted significantly the addition of the malonate onto the intact sidewall of SWNTs compared to the reaction at room temperature. On the contrary, more kinetically favorable products with Type 2 configurations than Type 1 configurations would be major on a theoretical basis of the Bingel reaction mechanism. As frequently seen for the isomerization of 6,5-open to 6,6-closed adducts of C_{60} by light and heat,[35,36,38] subsequent thermal rearrangements from Type 2 configuration to Type 1 may also be induced by the intensive direct heating of f-SWNT using the microwave reactor, which rationalizes the preservation of electronic structures of SWNTs after the reaction.

Conclusion

Details of structures, formation energies, and electronic properties of single-walled carbon nanotubes functionalized by Bingel reaction have been revealed by DFT calculations with finite-length nanotube models. The adducts with the binding configuration perpendicular to the tube axis (Type 1) exhibit the similar electronic structure to that of the pristine nanotubes due to the sidewall opening at the C–C bond between the bottom carbons. Selective formation of Type 1 configurations is consistent with the previous experimental results that the electronic properties of SWNTs are largely maintained.[29] At the current stage, real structures of covalently modified SWNTs cannot be determined experimentally because of the complex structures arising from difference in diameter, length, chirality, and defects. In this regard, it is highly valuable to speculate the bonding configurations by the combination of experimental and theoretical studies. Moreover, the investigations on the energy profiles of the transition states and the products reveal that the addition with Type 1 geometry is more exothermic but kinetically unfavorable compared to that with Type 2 geometry. This implies the occurrence of thermal isomerization from Type 2 to Type 1 after the Bingel reaction, allowing us to achieve the preservation of electronic structure as well as the excellent solubility of the covalently functionalized SWNTs. These results will provide an important clue in the design of functionalized carbon nanotubes that can exhibit both high processability and retention of favorable electronic properties.

Numerical calculations were partly performed at Research Center for Computational Science, Okazaki, Japan. H.I. thanks Grant-in-Aid from MEXT, Japan (Priority Area of Molecular Theory for Real Systems (No. 19029020)) for financial support. T.U. thanks Dr. Simon Mathew (Kyoto University) for valuable discussions.

Supporting Information

Optimized geometry of the (10,5) nanotube models, schematic energy profile, and structures of the transition states and the intermediate for the addition of $CCl(CO_2Me)_2^-$ to the (10,5) nanotube. These materials are available free of charge on the web at http://www.csj.jp/journals/bcsj/.

References

1 R. H. Baughman, A. A. Zakhidov, W. A. de Heer, *Science* **2002**, *297*, 787.
2 P. Avouris, Z. Chen, V. Perebeinos, *Nat. Nanotechnol.* **2007**, *2*, 605.
3 P. Avouris, M. Freitag, V. Perebeinos, *Nat. Photonics* **2008**, *2*, 341.
4 N. Karousis, N. Tagmatarchis, D. Tasis, *Chem. Rev.* **2010**, *110*, 5366.
5 X. Peng, S. S. Wong, *Adv. Mater.* **2009**, *21*, 625.
6 V. Georgakilas, K. Kordatos, M. Prato, D. M. Guldi, M. Holzinger, A. Hirsch, *J. Am. Chem. Soc.* **2002**, *124*, 760.
7 X. Lu, F. Tian, X. Xu, N. Wang, Q. Zhang, *J. Am. Chem. Soc.* **2003**, *125*, 10459.
8 E. Cho, S. Shin, Y.-G. Yoon, *J. Phys. Chem. C* **2008**, *112*, 11667.
9 J. L. Bahr, J. Yang, D. V. Kosynkin, M. J. Bronikowski, R. E. Smalley, J. M. Tour, *J. Am. Chem. Soc.* **2001**, *123*, 6536.
10 J.-x. Zhao, Y.-h. Ding, *J. Phys. Chem. C* **2008**, *112*, 13141.
11 J. Chen, M. A. Hamon, H. Hu, Y. Chen, A. M. Rao, P. C. Eklund, R. C. Haddon, *Science* **1998**, *282*, 95.
12 H. Hu, B. Zhao, M. A. Hamon, K. Kamaras, M. E. Itkis, R. C. Haddon, *J. Am. Chem. Soc.* **2003**, *125*, 14893.
13 K. Kamaras, M. E. Itkis, H. Hu, B. Zhao, R. C. Haddon, *Science* **2003**, *301*, 1501.
14 J. Zhao, Z. Chen, Z. Zhou, H. Park, P. R. Schleyer, J. P. Lu, *ChemPhysChem* **2005**, *6*, 598.
15 E. Cho, H. Kim, C. Kim, S. Han, *Chem. Phys. Lett.* **2006**,

419, 134.
16 H. F. Bettinger, *Chem.—Eur. J.* **2006**, *12*, 4372.
17 J. Lu, D. Wang, S. Nagase, M. Ni, X. Zhang, Y. Maeda, T. Wakahara, T. Nakahodo, T. Tsuchiya, T. Akasaka, Z. Gao, D. Yu, H. Ye, Y. Zhou, W. N. Mei, *J. Phys. Chem. B* **2006**, *110*, 5655.
18 Z. Chen, S. Nagase, A. Hirsch, R. C. Haddon, W. Thiel, P. R. Schleyer, *Angew. Chem., Int. Ed.* **2004**, *43*, 1552.
19 J. Li, G. Jia, Y. Zhang, Y. Chen, *Chem. Mater.* **2006**, *18*, 3579.
20 T. Fujigaya, N. Nakashima, *Polym. J.* **2008**, *40*, 577.
21 Y.-L. Zhao, J. F. Stoddart, *Acc. Chem. Res.* **2009**, *42*, 1161.
22 C.-Y. Hong, C.-Y. Pan, *J. Mater. Chem.* **2008**, *18*, 1831.
23 Y.-S. Lee, N. Marzari, *Phys. Rev. Lett.* **2006**, *97*, 116801.
24 A. López-Bezanilla, F. Triozon, S. Latil, X. Blase, S. Roche, *Nano Lett.* **2009**, *9*, 940.
25 C. Bingel, *Chem. Ber.* **1993**, *126*, 1957.
26 J.-F. Nierengarten, V. Gramlich, F. Cardullo, F. Diederich, *Angew. Chem., Int. Ed. Engl.* **1996**, *35*, 2101.
27 K. S. Coleman, S. R. Bailey, S. Fogden, M. L. H. Green, *J. Am. Chem. Soc.* **2003**, *125*, 8722.
28 K. A. Worsley, K. R. Moonoosawmy, P. Kruse, *Nano Lett.* **2004**, *4*, 1541.
29 T. Umeyama, N. Tezuka, M. Fujita, Y. Matano, N. Takeda, K. Murakoshi, K. Yoshida, S. Isoda, H. Imahori, *J. Phys. Chem. C* **2007**, *111*, 9734.
30 T. Yumura, M. Kertesz, *J. Phys. Chem. C* **2009**, *113*, 14184.
31 X. Gao, K. Ishimura, S. Nagase, Z. Chen, *J. Phys. Chem. A* **2009**, *113*, 3673.
32 R. Saito, G. Dresselhaus, M. S. Dresselhaus, *Physical Properties of Carbon Nanotubes*, Imperial College Press, London, **1998**.
33 M. J. Frisch, G. W. Trucks, H. B. Schlegel, G. E. Scuseria, M. A. Robb, J. R. Cheeseman, J. A. Montgomery, Jr., T. Vreven, K. N. Kudin, J. C. Burant, J. M. Millam, S. S. Iyengar, J. Tomasi, V. Barone, B. Mennucci, M. Cossi, G. Scalmani, N. Rega, G. A. Petersson, H. Nakatsuji, M. Hada, M. Ehara, K. Toyota, R. Fukuda, J. Hasegawa, M. Ishida, T. Nakajima, Y. Honda, O. Kitao, H. Nakai, M. Klene, X. Li, J. E. Knox, H. P. Hratchian, J. B. Cross, V. Bakken, C. Adamo, J. Jaramillo, R. Gomperts, R. E. Stratmann, O. Yazyev, A. J. Austin, R. Cammi, C. Pomelli, J. W. Ochterski, P. Y. Ayala, K. Morokuma, G. A. Voth, P. Salvador, J. J. Dannenberg, V. G. Zakrzewski, S. Dapprich, A. D. Daniels, M. C. Strain, O. Farkas, D. K. Malick, A. D. Rabuck, K. Raghavachari, J. B. Foresman, J. V. Ortiz, Q. Cui, A. G. Baboul, S. Clifford, J. Cioslowski, B. B. Stefanov, G. Liu, A. Liashenko, P. Piskorz, I. Komaromi, R. L. Martin, D. J. Fox, T. Keith, M. A. Al-Laham, C. Y. Peng, A. Nanayakkara, M. Challacombe, P. M. W. Gill, B. Johnson, W. Chen, M. W. Wong, C. Gonzalez, J. A. Pople, *Gaussian 03 (Revision E.01)*, Gaussian, Inc., Wallingford CT, **2004**.
34 M. Cossi, G. Scalmani, N. Rega, V. Barone, *J. Chem. Phys.* **2002**, *117*, 43.
35 L. Isaacs, A. Wehrsig, F. Diederich, *Helv. Chim. Acta* **1993**, *76*, 1231.
36 F. Diederich, L. Isaacs, D. Philp, *J. Chem. Soc., Perkin Trans. 2* **1994**, 391.
37 E. Vázquez, M. Prato, *ACS Nano* **2009**, *3*, 3819.
38 X. Xu, Z. Shang, G. Wang, Z. Cai, Y. Pan, X. Zhao, *J. Phys. Chem. A* **2002**, *106*, 9284.